

DRC001

Outside-the-loop Input Shaping with Quantitative Feedback Control for Flexible Systems Having Non-zero Initial Conditions

Withit Chatlatanagulchai^{1,*} and Dumrongsak Kijdech¹

¹ Control of Robot and Vibration Laboratory, Department of Mechanical Engineering, Faculty of Engineering, Kasetsart University, 50 Phahonyothin Rd., Chatuchak, Bangkok, 10900, Thailand

* Corresponding Author: fengwtc@ku.ac.th, Tel. +66-84-466-4472, Fax. +66-2-579-4576

Abstract

Input shaping is a technique to reduce residual vibration in point-to-point movement of flexible systems. The technique is based on destructive interference of impulse responses, that is, an impulse response can be cancelled by another impulse response, given appropriate impulse amplitudes and applied times. One of the assumptions used to develop the input shaper is zero initial conditions. Research work that considers non-zero initial conditions is almost non-existent. In some applications, such as emergency stop of a crane, we want to go from non-zero initial conditions to a complete stop of the crane. Besides, with input shaping or not, the flexible systems may not be completely still before the next maneuver is commenced. This paper shows that the non-zero initial conditions are equivalent to the plant-input disturbance. Quantitative feedback controller is placed inside the loop to reject this plant-input disturbance while the input shaper is placed outside the loop for suppressing reference induced vibration. Together, the proposed system effectively suppresses vibration induced by the non-zero initial conditions. A simulation on a two-mass rigid-flexible system confirms the effectiveness of the proposed system.

Keywords: Input shaping; Vibration reduction; Quantitative feedback control; Non-zero initial conditions.

1. Introduction

Input shaping is a technique to reduce residual vibration. The technique is based on destructive interference of impulse responses, that is, an impulse response can be cancelled by another impulse response, given appropriate impulse amplitudes and applied times.

Input shaping is designed based on an assumption that the flexible system has zero initial conditions before the next movement is commenced. However, in some applications such as emergency stop of a crane, it is required that the crane goes from non-zero initial conditions to a complete stop. Moreover, it should be expected that, even under input shaping, there still exists some leftover residual vibration from previous move cycle due to imperfect model, external disturbance, etc.

Research work on input shaping with flexible system having non-zero initial conditions is rare in the literature. Ref. [1] designs an input shaper analogous to that of the zero vibration (ZV) input shaper by taking into account the impulse response caused by the non-zero initial conditions. However, off-line experiments are required to determine the amplitude and phase shift parameters of the impulse response.

In this work, the input shaper is placed outside the loop. It will be shown that this input shaper can only suppress vibration induced by the reference signal and that the non-zero initial conditions can be thought of as plant-input disturbances. Inside the loop, a feedback controller is designed to reject the plant-input disturbances as well as to provide the closed-loop stability.

Simulation results on a two-mass rigid-flexible system show that the proposed control system

effectively suppress vibration induced by non-zero initial conditions.

This paper is organized in this way. Section 2 presents mathematical models of the two-mass rigid-flexible system. Section 3 contains details on input shaper used and shows via simulation the difficulty of the input shaper with systems having non-zero initial conditions. Section 4 accommodates the proposed technique. The input shaping with quantitative feedback control is discussed. Simulation results are given in Section 5 followed by conclusions in Section 6.

2. Two-mass Rigid-flexible System

Consider a two-mass rigid-flexible system in Fig. 1. In general, the system represents two entities, connected via a flexible part, which encompasses a large majority of actual rigid-flexible systems. The driving one has an absolute position and mass of x_0 and m_0 , and the driven one has x_1 and m_1 . k , c_0 , and c are spring stiffness and two damping constants. f is the control force. The objective is to move both masses from the origin to a displacement X with zero residual vibrations and in a shortest time possible T , that is,

$$\left. \begin{matrix} x_0 \\ x_1 \end{matrix} \right|_{t=T} = \begin{matrix} X \\ X \end{matrix}, \quad \left. \begin{matrix} \dot{x}_0 \\ \dot{x}_1 \end{matrix} \right|_{t=T} = \begin{matrix} 0 \\ 0 \end{matrix}.$$

DRC001

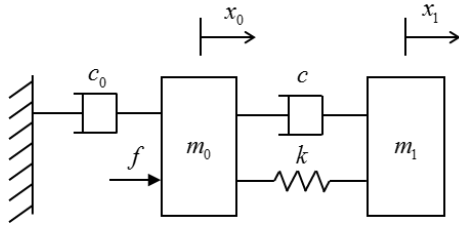


Fig. 1 Two-mass rigid-flexible system.

The equations of motion of the system in Fig. 1 can be found as

$$\begin{aligned} m_0 \ddot{x}_0 + c(\dot{x}_0 - \dot{x}_1) + k(x_0 - x_1) + c_0 \dot{x}_0 &= f, \\ m_1 \ddot{x}_1 - c(\dot{x}_0 - \dot{x}_1) - k(x_0 - x_1) &= 0. \end{aligned}$$

The corresponding state-space model with output x_1 is given by

$$\begin{aligned} \begin{Bmatrix} \dot{x}_0 \\ \ddot{x}_0 \\ \dot{x}_1 \\ \ddot{x}_1 \end{Bmatrix} &= \begin{bmatrix} 0 & 1 & 0 & 0 \\ \frac{k}{m_0} & -\frac{(c+c_0)}{m_0} & \frac{k}{m_0} & \frac{c}{m_0} \\ 0 & 0 & 0 & 1 \\ \frac{k}{m_1} & \frac{c}{m_1} & -\frac{k}{m_1} & -\frac{c}{m_1} \end{bmatrix} \begin{Bmatrix} x_0 \\ \dot{x}_0 \\ x_1 \\ \dot{x}_1 \end{Bmatrix} \\ + \begin{Bmatrix} 0 \\ \frac{1}{m_0} \\ 0 \\ 0 \end{Bmatrix} f, \quad y &= [0 \ 0 \ 1 \ 0]x. \end{aligned}$$

The corresponding transfer function from x_0 to x_1 is given by

$$P_2(s) = \frac{X_1(s)}{X_0(s)} = \frac{cs+k}{m_1 s^2 + cs+k},$$

and from f to x_0 is given by

$$\begin{aligned} P_1(s) &= \frac{X_0(s)}{F(s)} \\ &= \frac{m_1 s^2 + cs + k}{\left[m_0 m_1 s^4 + (m_0 c + m_1 c + m_1 c_0) s^3 \right. \\ &\quad \left. + (m_0 k + m_1 k + c c_0) s^2 + c_0 k s \right]}. \end{aligned}$$

Therefore, the transfer function from f to x_1 is given by

$$\begin{aligned} P_0(s) &= \frac{X_1(s)}{F(s)} \\ &= \frac{cs+k}{\left[m_0 m_1 s^4 + (m_0 c + m_1 c + m_1 c_0) s^3 \right. \\ &\quad \left. + (m_0 k + m_1 k + c c_0) s^2 + c_0 k s \right]}. \end{aligned} \quad (1)$$

In most rigid-flexible systems, such as cranes, the command input is velocity instead of acceleration or force. Therefore, from (1), the transfer function from the velocity command v to x_1 is given by

$$\begin{aligned} P(s) &= \frac{X_1(s)}{V(s)} \\ &= \frac{cs+k}{\left[m_0 m_1 s^3 + (m_0 c + m_1 c + m_1 c_0) s^2 \right. \\ &\quad \left. + (m_0 k + m_1 k + c c_0) s + c_0 k \right]}. \end{aligned} \quad (2)$$

For simulation purpose, let $m_0 = 2$ kg, $m_1 = 3$ kg, $c = 0.1$ kg.s⁻¹, $c_0 = 30$ kg.s⁻¹, and $k = 1$ kg.s⁻². The response x_1 from a unit-step velocity input v is shown in Fig. 2, where the effect of the flexible mode, with $\omega_n = 0.58$ rad.s⁻¹ and $\zeta = 5.8 \times 10^{-2}$, is evident.

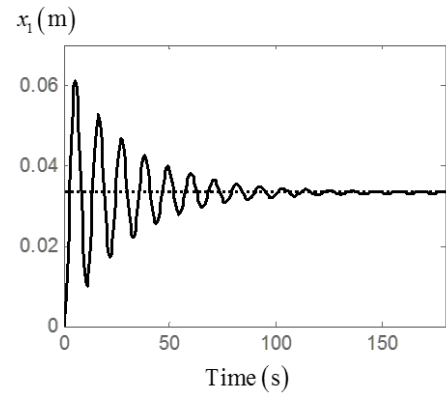


Fig. 2 Impulse response of the two-mass rigid-flexible system.

3. Input Shaping Problem with Non-zero Initial Conditions

This section presents a type of input shaper to be used in this work and illustrates via simulation the input shaping difficulty with systems having non-zero initial conditions.

3.1 Non-zero Initial Conditions as Plant-input Disturbance

Effect from non-zero initial conditions can be included in the plant-input disturbance as can be seen from the Laplace transformation of an underdamped plant with non-zero initial conditions given by

$$Y(s) = \frac{[F(s) + (ms+c)y(0) + m\dot{y}(0)]}{ms^2 + cs + k},$$

where $F(s)$ and $Y(s)$ are Laplace transforms of the input to and output from the system.

3.2 Zero Vibration and Derivative Input Shaper

Input shaping is based on destructive interference of impulse responses. A good tutorial paper is [2].

The ratio between the n -impulse response amplitude at time $t \geq t_n$ and the single-impulse response amplitude at time $t \geq t_1$ is given by

DRC001

$$V(\omega_n, \zeta) = e^{-\zeta\omega_n t_n} \sqrt{[C(\omega_n, \zeta)]^2 + [S(\omega_n, \zeta)]^2},$$

$$C(\omega_n, \zeta) = \sum_{i=1}^n A_i e^{\zeta\omega_n t_i} \cos(\omega_n \sqrt{1-\zeta^2} t_i),$$

$$S(\omega_n, \zeta) = \sum_{i=1}^n A_i e^{\zeta\omega_n t_i} \sin(\omega_n \sqrt{1-\zeta^2} t_i),$$

where V is the so-called *percentage vibration*, normally used in the literature to quantify the residual vibration, ω_n is the natural frequency of the applied linear system, ζ is its damping ratio, t_i is the time the i^{th} impulse is applied and A_i is the i^{th} impulse's amplitude.

The amplitudes A_i and time locations t_i of the impulse sequence are computed by solving the following equations:

$$V(\omega_n, \zeta) = 0, \quad (3)$$

$$\frac{\partial V(\omega_n, \zeta)}{\partial \omega_n} = 0, \quad (4)$$

$$\sum_{i=1}^n A_i = 1, \quad (5)$$

$$t_1 = 0, \quad (6)$$

which requires the knowledge of ω_n and ζ .

Eqs. (3) - (6) are used to solve six unknowns, which are the amplitudes and time locations of three impulses:

$$t_1 = 0, A_1 = \frac{1}{1+2K+K^2}, \quad (7)$$

$$t_2 = \frac{\pi}{\omega_n \sqrt{1-\zeta^2}}, A_2 = \frac{2K}{1+2K+K^2}, \quad (8)$$

$$t_3 = \frac{2\pi}{\omega_n \sqrt{1-\zeta^2}}, A_3 = \frac{K^2}{1+2K+K^2}, \quad (9)$$

$$K = e^{\frac{\zeta\pi}{\sqrt{1-\zeta^2}}}. \quad (10)$$

This three-impulse input shaper is known in the literature as zero vibration and derivative (ZVD) shaper. It was proposed by [3].

3.3 Open-loop Input Shaping

First, consider open-loop input shaping in Fig. 3, where IS represents the ZVD input shaper (7) - (10), P represents the flexible plant (2), v_b is the baseline velocity command (original command given by the operator), v is the shaped velocity command, and x_1 is the displacement of the mass m_1 .

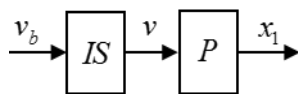


Fig. 3 Open-loop input shaping.

Without the input shaper, the response x_1 to a unit-step v_b is already shown in Fig. 2 in which excessive vibration is evident due to low level of damping.

Fig. 4 shows the simulation result when the input shaper is turned on for 20 seconds, off for the next 20 seconds, and on again for the remaining 60 seconds. Fig. 4(a) shows the baseline velocity command v_b . Fig. 4(b) contains the shaped velocity command v . Fig. 4(c) presents the displacement x_1 of mass m_1 .

The result in Fig. 4 can be explained in this way. For the first 20 seconds, the input shaper is turned on with zero initial conditions, so the displacement x_1 does not vibrate and can settle at a steady-state value. During the next 20 seconds, the input shaper is turned off, so the displacement x_1 vibrates and does not settle yet at the 40th second. Therefore, when the input shaper is turned back on again at the 40th second, the initial conditions are not yet zero. At this time, even though the input shaper can reduce some amount of vibration, it does not completely remove it. This simulation clearly shows the effect of non-zero initial conditions to the performance of the input shaper.

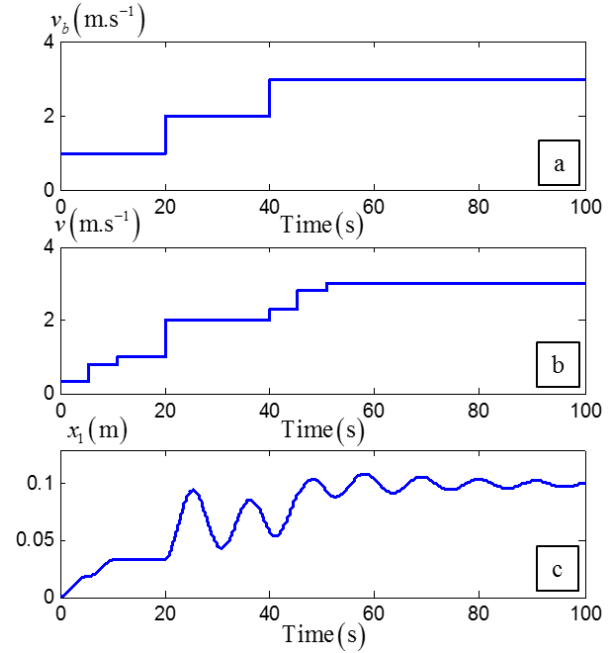


Fig. 4 Simulation result of open-loop input shaping. (a) Baseline velocity command v_b . (b) Shaped velocity command v . (c) Displacement x_1 of mass m_1 .

4. Input Shaping with Quantitative Feedback Control

This section presents the proposed system shown in Fig. 5, where F is the prefilter, G is the controller, d_i is the plant-input disturbance, d_o is the plant-output disturbance, and n is the noise. F and G will

DRC001

be designed using the quantitative feedback theory, whose details can be found in [4].

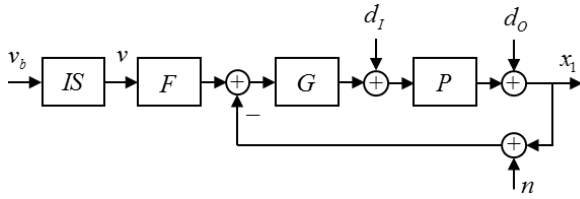


Fig. 5 Input shaping with quantitative feedback control.

The input shaper IS can suppress residual vibration induced by the reference input as can be seen from the transfer function from v_b to x_1 , which is given by

$$\frac{X_1(s)}{V_b(s)} = \frac{P(s)G(s)F(s)IS(s)}{1+P(s)G(s)},$$

where $IS(s)$ appears in the numerator.

However, the input shaper IS has no effect on the disturbances and noise. For example, the transfer function from d_I to x_1 , which is given by

$$\frac{X_1(s)}{D_I(s)} = \frac{P(s)}{1+P(s)G(s)},$$

has no input shaper IS in it.

Since the non-zero initial conditions can be thought of as the plant-input disturbance, the controller G must then be used to reject it.

5. Simulation Results

Consider the flexible plant (2). This section shows design of the proposed system in Fig. 5 that improves the performance of the system when non-zero initial conditions are present.

Assume that the two damping constants have $\pm 50\%$ uncertainties, that is, $c_0 \in \{0.05, 0.15\}$ and $c \in \{15, 45\}$.

The controller G will be designed for a plant-input disturbance rejection specification

$$\left| \frac{X_1(j\omega)}{D_I(j\omega)} \right| = \left| \frac{P(j\omega)}{1+P(j\omega)G(j\omega)} \right| < -30 \text{ dB}, \quad (11)$$

for $\omega \in \{0.05, 0.1, 0.2, 0.5, 0.8, 1\}$ rad/s. It will also be designed for a stability margin specification

$$\left| \frac{P(j\omega)G(j\omega)}{1+P(j\omega)G(j\omega)} \right| < 10 \text{ dB}, \quad (12)$$

for $\omega \in \{0.05, 0.1, 0.2, 0.5, 0.8, 1, 3, 7, 11\}$ rad/s. The frequencies of interest are around expected bandwidth of the system.

Note that the tracking specification is not imposed here because our attention is on rejecting the plant-input disturbance (non-zero initial conditions).

Note also that the stability margin specification (12) relates to the gain and phase margins according to the formulas

$$GM = 20 \log \left(\frac{M+1}{M} \right) \text{ dB},$$

$$PM = 2 \sin^{-1} \left(\frac{1}{2M} \right) \text{ rad},$$

where $M = 10^{10 \text{ dB}/20}$ in our case.

The controller G was found from loop-shaping to be

$$G = \frac{5531.9}{s^2 + 6.183s + 167.2}, \quad (13)$$

which consists of a gain and a pair of complex poles. The final open-loop shape as well as the combined bounds, representing the specifications (11) and (12), are shown in Fig. 6. The open-loop frequency responses $L(j\omega)$ for all frequencies of interest lie in the allowable regions.

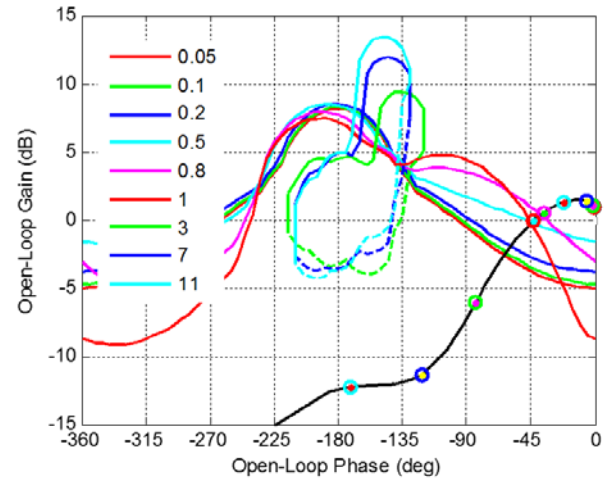


Fig. 6 Bounds on the Nichols chart and final loop shape $L(s) = G(s)P(s)$.

The prefilter F was set equal to one because no tracking specification was imposed.

The frequency-domain specifications (11) and (12) are simulated for 9 plant models spanning the uncertain sets of c_0 and c . The results are shown in Fig. 7, which shows that all specifications are met for all plant uncertainties.

DRC001

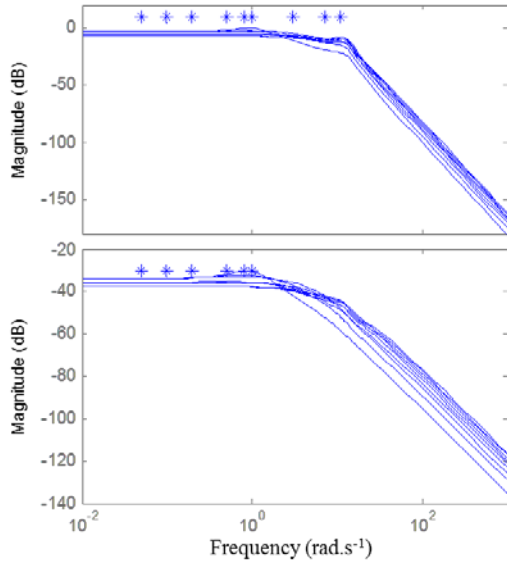


Fig. 7 Simulation results. (Top) $|PG / (1 + PG)|$. (Bottom) $|P / (1 + PG)|$. Asterisks mark corresponding bounds.

The closed-loop system in Fig. 5 is simulated with P as in (2), G as in (13), F as a unity, IS as in (7) - (10), and non-zero initial conditions. When the baseline velocity command v_b is a step function, the system output $y = x_1$ from the nominal plant is shown in Fig. 8(Bottom), whereas the baseline velocity command is shown in Fig. 8(Top) and the shaped velocity command is shown in Fig. 8(Middle).

It can be seen that the proposed system can reject the effect of the non-zero initial conditions well, allowing x_1 to reach its steady-state value without residual vibration.

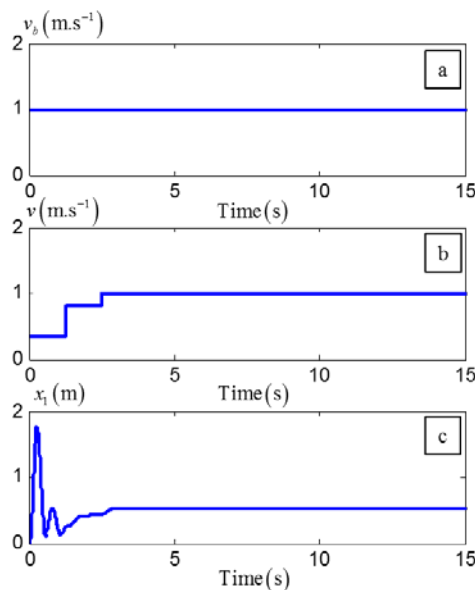


Fig. 8 Simulation result of input shaping with quantitative feedback control. (a) Baseline velocity command v_b . (b) Shaped velocity command v . (c) Displacement x_1 of mass m_1 .

Additional result on disturbance rejection is given in Fig. 9. Fig. 9(Top) shows the system output x_1 when the baseline velocity command v_b is zero and the plant-input disturbance d_I is a unit square wave. Fig. 9(Bottom) contains x_1 when v_b is zero and d_I is an impulse. It can be seen that the proposed system can reject the plant-input disturbance very well.

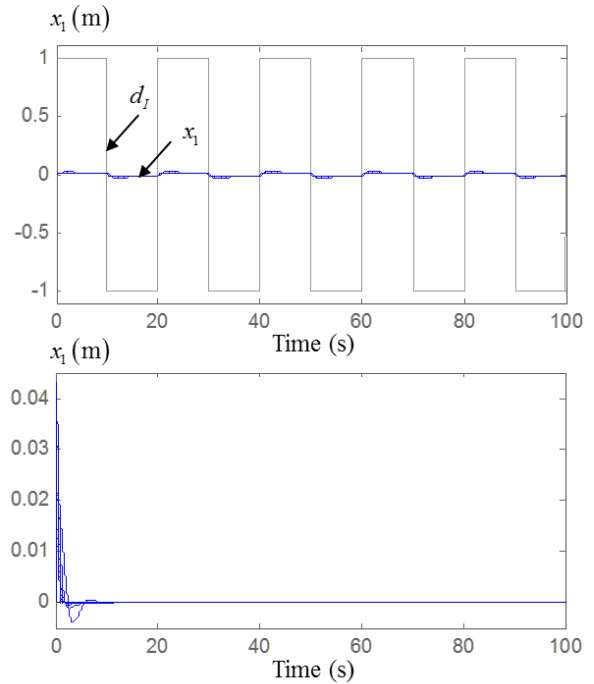


Fig. 9 System output x_1 . (Top) When plant-input disturbance d_I is a unit square wave. (Bottom) When d_I is an impulse.

Fig. 10 presents the result of using the proposed system, which is input shaping with quantitative feedback control. The figure is analogous to Fig. 4 when only the input shaper is used. At the 30th second, without input shaping, the system output x_1 is still vibrating when the input shaping is turned on with non-zero initial conditions. The system is able to reach a new steady-state value of 1.671 with a small amount of residual vibration even under the presence of non-zero initial conditions.

DRC001

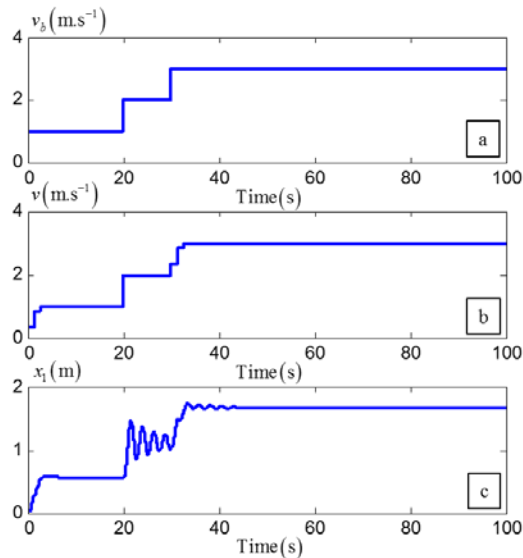


Fig. 10 Simulation result of input shaping with quantitative feedback control. (a) Baseline velocity command v_b . (b) Shaped velocity command v . (c) Displacement x_1 of mass m_1 .

6. Conclusions

Non-zero initial conditions are typically present in practice. Input shaping is designed by assuming zero initial conditions; therefore, its performance can deteriorate when non-zero initial conditions exist. Research work that considers this problem is rare.

In this paper, the input shaper is designed to work together with feedback control. The input shaper is placed outside to suppress vibration induced by the reference signal. The feedback control is designed to suppress vibration induced by the non-zero initial conditions. This can be done because the non-zero initial conditions are in fact the plant-input disturbances that can be rejected by the feedback controller.

Future work includes implementing the proposed technique with actual systems.

7. Acknowledgements

The authors would like to thank Craig Borghesani and Terasoft, Inc for their evaluation copy of the QFT Matlab toolbox.

8. References

- [1] Veciana, J.M., Cardona, S. and Català, P. (2013). Minimizing residual vibrations for non-zero initial states: application to an emergency stop of a crane, *International Journal of Precision Engineering and Manufacturing*, vol. 14(11), pp. 1901 – 1908.
- [2] Singhose, W. (2009). Command shaping for flexible systems: a review of the first 50 years, *International Journal of Precision Engineering and Manufacturing*, vol. 10(4), pp. 153 – 168.
- [3] Singer, N.C. and Seering, W.C. (1990). Preshaping command inputs to reduce system vibration, *ASME J.*

of Dynamics System, Measurement and Control, vol. 112(1), pp. 76 – 82.

[4] Yaniv, O. (1999). *Quantitative Feedback Design of Linear and Nonlinear Systems*, Kluwer Academic Publishers, Boston.